Inorganic Chemistry

pubs.acs.org/IC

Communication

Controlled Protonation of [2Fe−2S] Leading to MitoNEET Analogues and Concurrent Cluster Modification

Kady Oakley, Kevin Sterling, Jason Shearer, and Eunsuk Kim*

Cite This: *Inorg. Chem.* 2021, 60, 16074−16078

Read Online

ACCESS | Metrics & More | Article Recommendations | Supporting Information

ABSTRACT: MitoNEET, a key regulatory protein in mitochondrial energy metabolism, exhibits a uniquely ligated [2Fe−2S] cluster with one histidine and three cysteines. This unique cluster has been postulated to sense the redox environment and release Fe−S cofactors under acidic pH. Reported herein is a synthetic system that shows how [2Fe−2S] clusters react with protons and rearrange their coordination geometry. The low-temperature stable, site-differentiated clusters $[Fe_2S_2(SPh)_3(CF_3COO)]^{2-}$ and $[Fe_2S_2(SPh)_3(py)]^{-}$ have been prepared via controlled protonation below −35 °C and characterized by NMR, UV−vis, and X-ray absorption spectroscopy. Both complexes exhibit anodically shifted redox potentials compared to $[Fe_2S_2(SPh)_4]^{2-}$ and convert to $[Fe_4S_4(SPh)_4]^{2-}$ upon warming to room temperature. The current study provides insight into how mitoNEET releases its [2Fe−2S] in response to highly tuned acidic conditions, the chemistry of which may have further implications in Fe−S biogenesis.

Iron−sulfur (Fe−S) clusters are ubiquitous cofactors present in all animal kingdoms. Proteins containing [Fe−S] cofactors are essential to sustaining fundamental life processes such as respiration, metabolism, and gene regulation.[1] The biogenesis and trafficking of [Fe−S] clusters is a highly complex and coordinated process, the disruption of which can lead to a variety of diseases.[2] The most common structural types for [Fe−S] clusters are cysteine-ligated rhombic [2Fe−2S] and cubane [4Fe−4S] clusters in which [4Fe−4S] clusters are biosynthesized from [2Fe−2S] clusters.[2]

In 2004, a novel [2Fe−2S]-containing protein mitoNEET was discovered as an unintended target of a type 2 diabetes drug, pioglitazone.[3] Subsequent studies established that mitoNEET is an important protein in regulating mitochondrial functions and metabolism.[4] MitoNEET has quickly become a potential drug target for metabolic and neurodegenerative diseases including obesity, diabetes, cancer, and Parkinson's disease.[5] Crystallographic studies[6] reveal that mitoNEET is a dimeric protein, with each monomer hosting one [2Fe−2S] cluster. The [2Fe−2S] mitoNEET cluster has a unique coordination environment ligated by three cysteines (Cys) and one histidine (His) that is hydrogen-bonded to a nearby lysine through a conserved water molecule (Chart 1). Although the exact role of this [2Fe−2S] cluster remains unresolved, the unique histidine ligation is considered to be particularly important for the protein to respond to pH and redox changes.[7] Biochemical studies have shown that mitoNEET can transfer its [Fe−S] clusters to cytosolic proteins at acidic pH when the clusters are in the oxidized diferric state, which suggests that mitoNEET may act as a repair protein that can restore damaged iron−sulfur cofactors under oxidative stress.[5b,8] The known recipient proteins identified from *in vitro* biochemical studies include [2Fe−2S] accepting apoferredoxin,[8a−c] anamorsin,[8d] and [4Fe−4S]-accepting iron regulatory protein.[5b] Alternatively, mitoNEET has also been suggested as an electron-transfer protein that can enhance glycolysis in the cytosol by promoting oxidation of NADH.[9]

Chart 1. X-ray Structure of mitoNEET (PDB 2QH7) and Synthetic Models

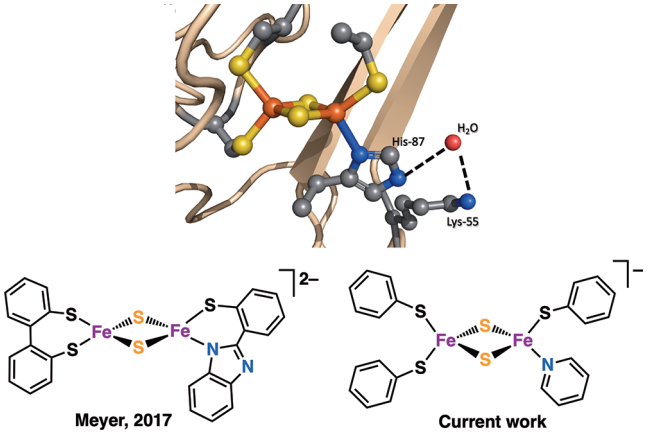

Synthetically modeling the [2Fe−2S] cluster in mitoNEET has been challenging given its unique 3Cys−His ligation. In 2017, Meyer and co-workers reported the first and only synthetic mitoNEET model complex (Chart 1), which demonstrated how the nitrogen-bound site allows for proton-coupled electron transfer.[10] Herein we report a new synthetic strategy to achieve site-differentiated [2Fe−2S] clusters assisted by controlled protonation, which allows for efficient

Received: August 24, 2021
Published: October 21, 2021

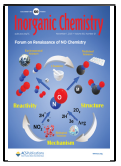

https://doi.org/10.1021/acs.inorgchem.1c02622
Inorg. Chem. 2021, 60, 16074−16078

product formation with the potential for ligand modification. Our model compound bears a neutral nitrogen-donor ligand (Chart 1), which can serve as a synthetic model for the unstable mitoNEET intermediate en route to cluster transfer. We also report the [2Fe−2S]-to-[4Fe−4S] cluster transformation induced by proton delivery to [2Fe−2S] clusters without introducing an external reductant. This lays an additional chemical foundation for studies in the area of [Fe−S] biogenesis in general.

Our initial attempts to synthesize site-differentiated [2Fe−2S] clusters by simple ligand substitution often led to the formation of homoleptic sulfur-ligated [2Fe−2S] clusters with a varying degree of decomposition. This synthetic challenge led us to seek out a way to remove one of the thiolate ligands from $(NEt_4)_2[Fe_2S_2(SPh)_4]$ (**1**) without introducing a strong incoming ligand. It is documented that **1** is unstable in aqueous or protic solvents in which **1** slowly converts to a tetranuclear cluster, $[Fe_4S_4(SPh)_4]^{2-}$, over 12−24 h by an unknown mechanism.[11] We thought protonation would be a key step in disrupting the coordination environment of **1**. Upon the addition of 1 equiv of trifluoroacetic acid (TFA) to **1** at −60 °C in a solvent mixture of acetonitrile-d_3 and *N*,*N*-dimethylformamide (DMF)-d_7 (1:3, v/v), noticeable changes were observed in ^{1}H NMR spectra (Figures 1 and S1). The

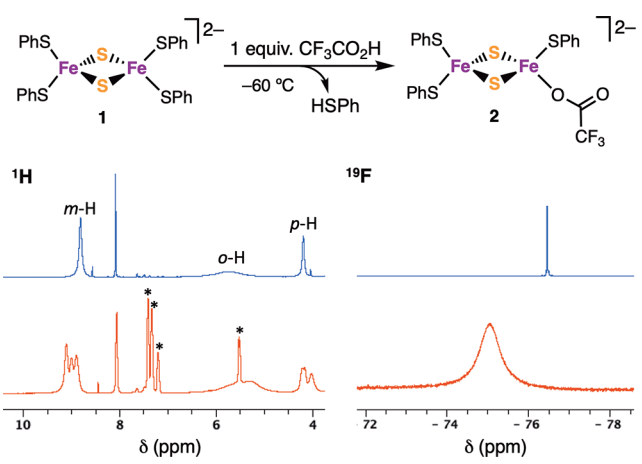

Figure 1. (Left) ^{1}H NMR spectra of **1** before (blue) and after (red) the addition of 1 equiv of TFA at −60 °C in 1:3 CD_3CN/DMF-d_7, generating **2** and the evolution of thiophenol (*). (Right) ^{19}F NMR spectra of TFA before (blue) the addition to **1** to generate **2** (red) at −60 °C in 1:3 CD_3CN/DMF-d_7.

compound remains diamagnetic during the reaction, but the *m*- and *p*-hydrogen resonances of the thiophenolate ligands exhibit splitting patterns after the acid treatment. Additionally, the reaction concomitantly generates 1 equiv of free thiophenol. This suggests that the acid treatment breaks the symmetry of **1** by protonating off one thiophenolate ligand, while maintaining the antiferromagnetically coupled [2Fe−2S] core structure. The resulting [2Fe−2S] cluster is stabilized by a new anionic ligand, trifluoroacetate, to form $(NEt_4)_2[Fe_2S_2(SPh)_3(CF_3CO_2)]$ (**2**). Coordination of trifluoroacetate to iron was confirmed by ^{19}F NMR spectroscopy in which the significantly broadened fluorine signal from **2** appears at −75.1 ppm, in contrast to a sharp signal for free TFA at −76.5 ppm (Figure 1).

We investigated the reversibility of this acid-induced ligand substitution by UV−vis monitoring at −80 °C in propionitrile. The UV−vis spectra of **1** and **2** are similar to each other, analogous to the similar visible absorption spectra observed from mitoNEET and its H87C mutant.[7d] However, the formation of **2** can still be seen in the decrease of the S → Fe charge-transfer band[12] at 500 nm by ∼15% upon the addition of 1 equiv of TFA. Nearly full recovery of **1** is obtained when 1 equiv of thiophenolate is added back to the solution (Figure S9). The addition of thiolate back to **2** also abolishes the subsequent reactivity unique to **2** (*vide infra*). This suggests that the trifluoroacetate ligand in **2** is poised for further substitution and **2** can serve as a precursor to other singly substituted [2Fe−2S] clusters.

We next sought to replace the ligated trifluoroacetate of **2** with a nitrogen-donor ligand to model a monodentate, single-substituted mitoNEET [2Fe−2S] cluster. We were able to achieve such a reaction by employing excess (≥50 equiv) pyridine (py) as an incoming ligand to form $(NEt_4)[Fe_2S_2(SPh)_3(py)]$ (**3**). The release of trifluoroacetate was observed by ^{19}F NMR spectroscopy when excess py was added to **2** in DMF-d_7 at −35 °C, in which the broad ^{19}F signal at −75.1 ppm from **2** immediately disappears with an emergence of a sharp singlet at −74.5 ppm that matches with the signal from authentic $[NEt_4][CF_3CO_2]$ (Figures S2 and S3). Compound **3** can also be prepared *in situ* by treating a solution of **1** (in DMF or acetonitrile) with 1 equiv of TFA dissolved in py. The ^{1}H NMR spectrum of **3** shows splitting of the *m*- and *p*-hydrogen resonances of the thiophenolate ligands, indicative of the asymmetric nature of a single-substituted [2Fe−2S] cluster (Figure S2). The effect of ligand substitution on the electrochemical properties were studied by cyclic voltammetry at −35 °C in CH_3CN (Figure S8). Compound **1** in 0.1 M NBu_4PF_6 exhibits an irreversible reduction peak potential at −1.48 V versus Fc^+/Fc, which is shifted to −1.27 V upon substitution of thiophenolate with trifluoroacetate. Further conversion from **2** to **3** leads to a new irreversible reduction peak at −1.39 V. This observed potential shift is in line with the electron-donating ability of the ligands with an order of thiolate > pyridine > trifluoroacetate. A similar redox potential trend by this set of ligands was previously shown with an oxoiron(IV) porphyrin complex.[13] The anodically shifted peak potentials of **2** and **3** suggest that the single-substituted complexes are more easily reduced compared to the homoleptic cluster **1**.

The three [2Fe−2S] clusters were probed by Fe K-edge X-ray absorption spectroscopy (XAS). All three complexes display an edge position consistent with the formal Fe^{3+} oxidation state and a prominent peak in the preedge region indicative of pseudotetrahedral iron (Figure S5). As expected, the extended X-ray absorption fine structure (EXAFS) region of the Fe K-edge XAS spectrum for **1** is best modeled as a four-coordinate iron center with four sulfur scatterers at 2.27 Å and an outer-sphere Fe···Fe vector at 2.71 Å (Figure 2).[14] Upon conversion of **1** to **2**, the EXAFS-derived average Fe···Fe and Fe−S vectors remain virtually unchanged at 2.71 and 2.28 Å, respectively. However, the model for the data indicate that the number of sulfur scatterers has decreased (i.e., the model required a decrease in N or an increase in σ^2), with the reported fit to the data employing 3.5 Fe−S scatterers. In addition, a Fe−O vector, modeled with 0.5 scatterers, is now located at 1.99 Å, indicating the coordination of trifluoroacetate to one of the iron centers. Conversion of **2** into **3** yields a further change to the EXAFS. Although the Fe···Fe and Fe−S vectors remain virtually unchanged (R_{Fe-S} = 2.27 Å;

https://doi.org/10.1021/acs.inorgchem.1c02622
Inorg. Chem. 2021, 60, 16074−16078

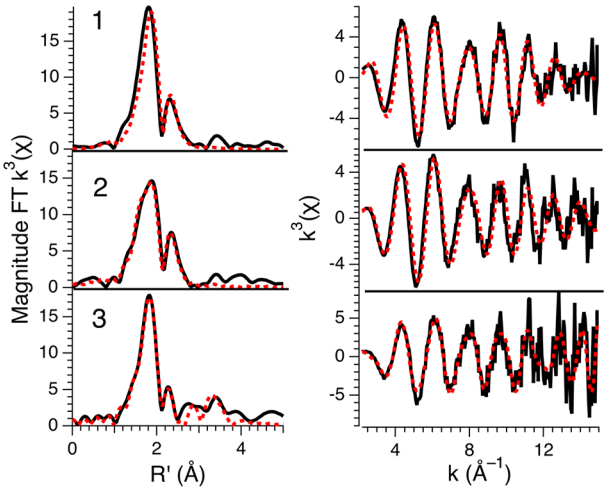

Figure 2. Magnitude Fourier-transformed $k^3(\chi)$ (left) and unfiltered $k^3(\chi)$ data for complexes **1** (top), **2** (middle), and **3** (bottom). The experimental data are given as solid black spectra, while the best fit to the data are given as dashed red spectra.

R_{Fe-Fe} = 2.70 Å), the inner-sphere light-atom scattering pathway, now modeled as a nitrogen atom, elongates to 2.20 Å. Furthermore, shells for outer-sphere carbon atoms at 3.31 and 3.9 Å now must be included in the model to adequately fit the data. These results indicate displacement of the trifluoroacetate ligand in **2** with a py ligand in **3**. The observed bond vectors in **3** compare well with the Fe−N (2.18−2.22 Å), Fe−S (2.21−2.36 Å), and Fe−Fe (2.74−2.75 Å) bond distances from the reported crystal structure of human mitoNEET in the oxidized state.[6b]

Complexes **2** and **3** are stable in solution below −35 °C. However, both complexes converted to a [4Fe-4S] cluster, $(NEt_4)_2[Fe_4S_4(SPh)_4]$ (**4**), upon warming to room temperature (Scheme 1). Dimerization of 2 equiv of diferric $[Fe_2S_2]^{2+}$

Scheme 1

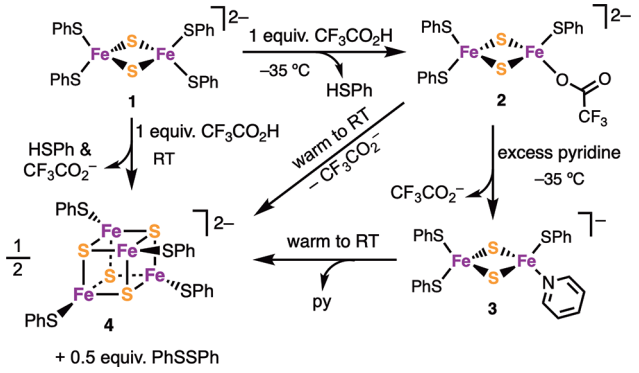

to form a mixed-valent (MV) $[Fe_4S_4]^{2+}$ cluster requires a reduction of iron by two electrons. The ^{1}H NMR spectra of the product mixtures after **2** or **3** was brought to room temperature showed the generation of phenyl disulfide, which suggests that the necessary electrons for cluster conversion came from their own thiophenolate ligands.

The acid-induced [2Fe−2S]-to-[4Fe−4S] conversion was further investigated at room temperature to examine whether stabilization of **2** or **3** is necessary for cluster conversion. A clean and immediate formation of **4** was observed when **1** was treated with 1 equiv of TFA at room temperature, which was accompanied by stoichiometric amounts of phenyl disulfide and free thiophenol generation (Figure 3). To examine the

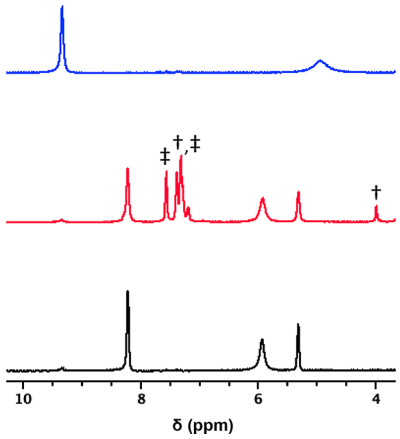

Figure 3. ^{1}H NMR spectra (room temperature, CD_3CN) of **1** before (blue) and after (red) the addition of 1 equiv of TFA compared to authentic **4** (black): †thiol and ‡disulfide formation.

generality of the reaction, we further investigated the ability of different acids to induce the cluster conversion. Compound **1** was exposed to 1 equiv of acetic acid (AA), TFA, or *p*-toluenesulfonic acid (PTSA), and the formation of **4** was analyzed by ^{1}H NMR spectroscopy, where pK_a values of AA, TFA, and PTSA are 23.51, 12.61, and 8.45 in CH_3CN,[15] respectively. The acid strength plays a significant role in the efficacy of the reaction. While the formation of **4** from **1** was quantitative with TFA, an incomplete conversion (28% yield) was observed with a weaker acid, AA, and a substantial amount of decomposed product was observed with a stronger acid, PTSA (Figure S7).

It is well-known that the reduction of diferric $[Fe_2S_2]^{2+}$ to MV $[Fe_2S_2]^{+}$ by an outer-sphere reductant leads to dimerization to form a MV cubane $[Fe_4S_4]^{2+}$ cluster.[16] Our results show that the same type of cluster transformation can be efficiently achieved by delivering a proton to the $[Fe_2S_2]^{2+}$ site, which promotes an internal electron transfer from the thiolate ligand to the cluster (Scheme 2). This transformation

Scheme 2

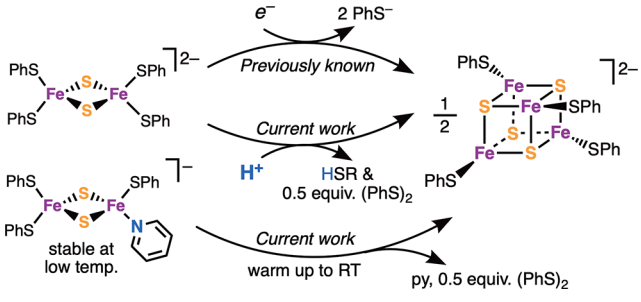

also indicates that the delivery of a proton to a single anionic ligand of the [2Fe−2S] cluster not only removes the targeted ligand by protonation but also induces a reductive bond cleavage of another iron−thiolate bond. Given that cluster release from oxidized mitoNEET is triggered by the protonation of His-87, it is conceivable that a similar type of Fe−Cys bond cleavage might occur when mitoNEET loses its cluster upon protonation.

https://doi.org/10.1021/acs.inorgchem.1c02622
Inorg. Chem. 2021, 60, 16074−16078

In summary, we have described a new synthetic strategy for site-differentiated [2Fe−2S] clusters. With this method, **3** has been prepared to model the pH- and redox-sensing [2Fe−2S] mitoNEET cluster. Introducing a py substituent or direct protonation of **1** induces reductive cleavage of a Fe−S(thiolate) bond and cluster dimerization to produce **4** with liberation of disulfide.

■ ASSOCIATED CONTENT

Supporting Information

The Supporting Information is available free of charge at https://pubs.acs.org/doi/10.1021/acs.inorgchem.1c02622.

Experimental details, spectroscopic (^{1}H and ^{19}F NMR, UV−vis, and XAS) data, and cyclic voltammograms (PDF)

■ AUTHOR INFORMATION

Corresponding Author

Eunsuk Kim − *Department of Chemistry, Brown University, Providence, Rhode Island 02912, United States;* orcid.org/0000-0001-8803-0666; Email: eunsuk_kim@brown.edu

Authors

Kady Oakley − *Department of Chemistry, Brown University, Providence, Rhode Island 02912, United States*

Kevin Sterling − *Department of Chemistry, Brown University, Providence, Rhode Island 02912, United States*

Jason Shearer − *Department of Chemistry, Trinity University, San Antonio, Texas 78212, United States;* orcid.org/0000-0001-7469-7304

Complete contact information is available at: https://pubs.acs.org/10.1021/acs.inorgchem.1c02622

Notes

The authors declare no competing financial interest.

■ ACKNOWLEDGMENTS

Financial support for this work was provided by the NSF (Grants CHE-1807845 and CHE-1854854) and NIH (Grants R15 CA213042 and GM120641-01).

■ REFERENCES

(1) Johnson, D. C.; Dean, D. R.; Smith, A. D.; Johnson, M. K. Structure, function, and formation of biological iron-sulfur clusters. *Annu. Rev. Biochem.* **2005**, *74*, 247−281.

(2) (a) Ciofi-Baffoni, S.; Nasta, V.; Banci, L. Protein networks in the maturation of human iron-sulfur proteins. *Metallomics* **2018**, *10*, 49−72. (b) Wachnowsky, C.; Fidai, I.; Cowan, J. A. Iron-sulfur cluster biosynthesis and trafficking - impact on human disease conditions. *Metallomics* **2018**, *10*, 9−29.

(3) Colca, J. R.; McDonald, W. G.; Waldon, D. J.; Leone, J. W.; Lull, J. M.; Bannow, C. A.; Lund, E. T.; Mathews, W. R. Identification of a novel mitochondrial protein ("mitoNEET") cross-linked specifically by a thiazolidinedione photoprobe. *Am. J. Physiol. Endocrinol. Metab.* **2004**, *286*, E252−260.

(4) (a) Tamir, S.; Paddock, M. L.; Darash-Yahana-Baram, M.; Holt, S. H.; Sohn, Y. S.; Agranat, L.; Michaeli, D.; Stofleth, J. T.; Lipper, C. H.; Morcos, F.; Cabantchik, I. Z.; Onuchic, J. N.; Jennings, P. A.; Mittler, R.; Nechushtai, R. Structure-function analysis of NEET proteins uncovers their role as key regulators of iron and ROS homeostasis in health and disease. *Biochim. Biophys. Acta, Mol. Cell Res.* **2015**, *1853*, 1294−1315. (b) Mittler, R.; Darash-Yahana, M.; Sohn, Y. S.; Bai, F.; Song, L.; Cabantchik, I. Z.; Jennings, P. A.; Onuchic, J. N.; Nechushtai, R. NEET Proteins: A New Link Between Iron Metabolism, Reactive Oxygen Species, and Cancer. *Antioxid. Redox Signaling* **2019**, *30*, 1083−1095.

(5) (a) Kusminski, C. M.; Holland, W. L.; Sun, K.; Park, J.; Spurgin, S. B.; Lin, Y.; Askew, G. R.; Simcox, J. A.; McClain, D. A.; Li, C.; Scherer, P. E. MitoNEET-driven alterations in adipocyte mitochondrial activity reveal a crucial adaptive process that preserves insulin sensitivity in obesity. *Nat. Med.* **2012**, *18*, 1539−1549. (b) Ferecatu, I.; Goncalves, S.; Golinelli-Cohen, M. P.; Clemancey, M.; Martelli, A.; Riquier, S.; Guittet, E.; Latour, J. M.; Puccio, H.; Drapier, J. C.; Lescop, E.; Bouton, C. The diabetes drug target MitoNEET governs a novel trafficking pathway to rebuild an Fe-S cluster into cytosolic aconitase/iron regulatory protein 1. *J. Biol. Chem.* **2014**, *289*, 28070−28086. (c) Sohn, Y. S.; Tamir, S.; Song, L.; Michaeli, D.; Matouk, I.; Conlan, A. R.; Harir, Y.; Holt, S. H.; Shulaev, V.; Paddock, M. L.; Hochberg, A.; Cabanchick, I. Z.; Onuchic, J. N.; Jennings, P. A.; Nechushtai, R.; Mittler, R. NAF-1 and mitoNEET are central to human breast cancer proliferation by maintaining mitochondrial homeostasis and promoting tumor growth. *Proc. Natl. Acad. Sci. U. S. A.* **2013**, *110*, 14676−14681. (d) Geldenhuys, W. J.; Benkovic, S. A.; Lin, L.; Yonutas, H. M.; Crish, S. D.; Sullivan, P. G.; Darvesh, A. S.; Brown, C. M.; Richardson, J. R. MitoNEET (CISD1) Knockout Mice Show Signs of Striatal Mitochondrial Dysfunction and a Parkinson's Disease Phenotype. *ACS Chem. Neurosci.* **2017**, *8*, 2759−2765.

(6) (a) Paddock, M. L.; Wiley, S. E.; Axelrod, H. L.; Cohen, A. E.; Roy, M.; Abresch, E. C.; Capraro, D.; Murphy, A. N.; Nechushtai, R.; Dixon, J. E.; Jennings, P. A. MitoNEET is a uniquely folded 2Fe2S outer mitochondrial membrane protein stabilized by pioglitazone. *Proc. Natl. Acad. Sci. U. S. A.* **2007**, *104*, 14342−14347. (b) Lin, J.; Zhou, T.; Ye, K.; Wang, J. Crystal structure of human mitoNEET reveals distinct groups of iron sulfur proteins. *Proc. Natl. Acad. Sci. U. S. A.* **2007**, *104*, 14640−14645. (c) Lipper, C. H.; Karmi, O.; Sohn, Y. S.; Darash-Yahana, M.; Lammert, H.; Song, L.; Liu, A.; Mittler, R.; Nechushtai, R.; Onuchic, J. N.; Jennings, P. A. Structure of the human monomeric NEET protein MiNT and its role in regulating iron and reactive oxygen species in cancer cells. *Proc. Natl. Acad. Sci. U. S. A.* **2018**, *115*, 272−277. (d) Geldenhuys, W. J.; Long, T. E.; Saralkar, P.; Iwasaki, T.; Nunez, R. A. A.; Nair, R. R.; Konkle, M. E.; Menze, M. A.; Pinti, M. V.; Hollander, J. M.; Hazlehurst, L. A.; Robart, A. R. Crystal structure of the mitochondrial protein mitoNEET bound to a benzenesulfonide ligand. *Commun. Chem.* **2019**, *2*, 77.

(7) (a) Conlan, A. R.; Axelrod, H. L.; Cohen, A. E.; Abresch, E. C.; Zuris, J.; Yee, D.; Nechushtai, R.; Jennings, P. A.; Paddock, M. L. Crystal structure of Miner1: The redox-active 2Fe-2S protein causative in Wolfram Syndrome 2. *J. Mol. Biol.* **2009**, *392*, 143−153. (b) Bak, D. W.; Elliott, S. J. Conserved hydrogen bonding networks of MitoNEET tune Fe-S cluster binding and structural stability. *Biochemistry* **2013**, *52*, 4687−4696. (c) Bak, D. W.; Zuris, J. A.; Paddock, M. L.; Jennings, P. A.; Elliott, S. J. Redox characterization of the FeS protein MitoNEET and impact of thiazolidinedione drug binding. *Biochemistry* **2009**, *48*, 10193−10195. (d) Wiley, S. E.; Paddock, M. L.; Abresch, E. C.; Gross, L.; van der Geer, P.; Nechushtai, R.; Murphy, A. N.; Jennings, P. A.; Dixon, J. E. The outer mitochondrial membrane protein mitoNEET contains a novel redox-active 2Fe-2S cluster. *J. Biol. Chem.* **2007**, *282*, 23745−23749.

(8) (a) Zuris, J. A.; Harir, Y.; Conlan, A. R.; Shvartsman, M.; Michaeli, D.; Tamir, S.; Paddock, M. L.; Onuchic, J. N.; Mittler, R.; Cabantchik, Z. I.; Jennings, P. A.; Nechushtai, R. Facile transfer of [2Fe-2S] clusters from the diabetes drug target mitoNEET to an apo-acceptor protein. *Proc. Natl. Acad. Sci. U. S. A.* **2011**, *108*, 13047−13052. (b) Golinelli-Cohen, M. P.; Lescop, E.; Mons, C.; Goncalves, S.; Clemancey, M.; Santolini, J.; Guittet, E.; Blondin, G.; Latour, J. M.; Bouton, C. Redox Control of the Human Iron-Sulfur Repair Protein MitoNEET Activity via Its Iron-Sulfur Cluster. *J. Biol. Chem.* **2016**, *291*, 7583−7593. (c) Mons, C.; Botzanowski, T.; Nikolaev, A.; Hellwig, P.; Cianferani, S.; Lescop, E.; Bouton, C.; Golinelli-Cohen, M. P. The H_2O_2-Resistant Fe-S Redox Switch MitoNEET Acts as a pH Sensor To Repair Stress-Damaged Fe-S Protein. *Biochemistry* **2018**, *57*, 5616−5628. (d) Lipper, C. H.; Paddock, M. L.; Onuchic, J.

N.; Mittler, R.; Nechushtai, R.; Jennings, P. A. Cancer-Related NEET Proteins Transfer 2Fe-2S Clusters to Anamorsin, a Protein Required for Cytosolic Iron-Sulfur Cluster Biogenesis. *PLoS One* **2015**, *10*, No. e0139699.

(9) (a) Wang, Y.; Landry, A. P.; Ding, H. The mitochondrial outer membrane protein mitoNEET is a redox enzyme catalyzing electron transfer from FMNH2 to oxygen or ubiquinone. *J. Biol. Chem.* **2017**, *292*, 10061−10067. (b) Li, X.; Wang, Y.; Tan, G.; Lyu, J.; Ding, H. Electron transfer kinetics of the mitochondrial outer membrane protein mitoNEET. *Free Radical Biol. Med.* **2018**, *121*, 98−104. (c) Tasnim, H.; Landry, A. P.; Fontenot, C. R.; Ding, H. Exploring the FMN binding site in the mitochondrial outer membrane protein mitoNEET. *Free Radical Biol. Med.* **2020**, *156*, 11−19.

(10) Bergner, M.; Dechert, S.; Demeshko, S.; Kupper, C.; Mayer, J. M.; Meyer, F. Model of the MitoNEET [2Fe-2S] Cluster Shows Proton Coupled Electron Transfer. *J. Am. Chem. Soc.* **2017**, *139*, 701−707.

(11) (a) Cambray, J.; Lane, R. W.; Wedd, A. G.; Johnson, R. W.; Holm, R. H. Chemical and Electrochemical Interrelationships of 1-Fe, 2-Fe, and 4-Fe Analogs of Active-Sites of Iron-Sulfur Proteins. *Inorg. Chem.* **1977**, *16*, 2565−2571. (b) Hagen, K. S.; Reynolds, J. G.; Holm, R. H. Definition of Reaction Sequences Resulting in Self-Assembly of $[Fe_4S_4(SR)_4]^{2-}$ Clusters from Simple Reactants. *J. Am. Chem. Soc.* **1981**, *103*, 4054−4063.

(12) (a) Blum, H.; Adar, F.; Salerno, J. C.; Leigh, J. S. Exchange Coupling in Spinach Ferredoxin Determined by Resonance Raman-Spectroscopy. *Biochem. Biophys. Res. Commun.* **1977**, *77*, 650−657. (b) Noodleman, L.; Baerends, E. J. Electronic-Structure, Magnetic-Properties, Electron-Spin-Resonance, and Optical-Spectra for 2-Fe Ferredoxin Models by Lcao-X-Alpha Valence Bond Theory. *J. Am. Chem. Soc.* **1984**, *106*, 2316−2327. (c) Chilkuri, V. G.; DeBeer, S.; Neese, F. Ligand Field Theory and Angular Overlap Model Based Analysis of the Electronic Structure of Homovalent Iron-Sulfur Dimers. *Inorg. Chem.* **2020**, *59*, 984−995.

(13) Takahashi, A.; Kurahashi, T.; Fujii, H. Redox potentials of oxoiron(IV) porphyrin pi-cation radical complexes: participation of electron transfer process in oxygenation reactions. *Inorg. Chem.* **2011**, *50*, 6922−6928.

(14) The sulfur shell can be divided into two shells containing two sulfur scatterers each at 2.34 and 2.24 Å; however, ΔR between the two shells is less than the resolution of the data of ΔR = 0.12 Å.

(15) Kutt, A.; Leito, I.; Kaljurand, I.; Soovali, L.; Vlasov, V. M.; Yagupolskii, L. M.; Koppel, I. A. A comprehensive self-consistent spectrophotometric acidity scale of neutral Brønsted acids in acetonitrile. *J. Org. Chem.* **2006**, *71*, 2829−2838.

(16) Holm, R. H.; Lo, W. Structural Conversions of Synthetic and Protein-Bound Iron-Sulfur Clusters. *Chem. Rev.* **2016**, *116*, 13685−13713.

https://doi.org/10.1021/acs.inorgchem.1c02622
Inorg. Chem. 2021, 60, 16074−16078